ELSEVIER

Biophysical Chemistry 121 (2006) 194–208

Biophysical Chemistry

http://www.elsevier.com/locate/biophyschem

Spatial modeling of dimerization reaction dynamics in the plasma membrane: Monte Carlo vs. continuum differential equations

Kapil Mayawala [a], Dionisios G. Vlachos [a,*], Jeremy S. Edwards [b,*]

[a] *Department of Chemical Engineering, 150 Academy Street, University of Delaware, Newark, DE 19716, USA*
[b] *Molecular Genetics and Microbiology, Cancer Research and Treatment Center, University of New Mexico Health Sciences Center, and Chemical and Nuclear Engineering, University of New Mexico, Albuquerque, NM 87131, USA*

Received 14 January 2006; accepted 19 January 2006
Available online 28 February 2006

Abstract

Bimolecular reactions in the plasma membrane, such as receptor dimerization, are a key signaling step for many signaling systems. For receptors to dimerize, they must first diffuse until a collision happens, upon which a dimerization reaction may occur. Therefore, study of the dynamics of cell signaling on the membrane may require the use of a spatial modeling framework. Despite the availability of spatial simulation methods, e.g., stochastic spatial Monte Carlo (MC) simulation and partial differential equation (PDE) based approaches, many biological models invoke well-mixed assumptions without completely evaluating the importance of spatial organization. Whether one is to utilize a spatial or non-spatial simulation framework is therefore an important decision. In order to evaluate the importance of spatial effects a priori, i.e., without performing simulations, we have assessed the applicability of a dimensionless number, known as second Damköhler number (*Da*), defined here as the ratio of time scales of collision and reaction, for 2-dimensional bimolecular reactions. Our study shows that dimerization reactions in the plasma membrane with $Da \sim > 0.1$ (tested in the receptor density range of 10^2–$10^5/\mu m^2$) require spatial modeling. We also evaluated the effective reaction rate constants of MC and simple deterministic PDEs. Our simulations show that the effective reaction rate constant decreases with time due to time dependent changes in the spatial distribution of receptors. As a result, the effective reaction rate constant of simple PDEs can differ from that of MC by up to two orders of magnitude. Furthermore, we show that the fluctuations in the number of copies of signaling proteins (noise) may also depend on the diffusion properties of the system. Finally, we used the spatial MC model to explore the effect of plasma membrane heterogeneities, such as receptor localization and reduced diffusivity, on the dimerization rate. Interestingly, our simulations show that localization of epidermal growth factor receptor (EGFR) can cause the diffusion limited dimerization rate to be up to two orders of magnitude higher at higher average receptor densities reported for cancer cells, as compared to a normal cell.

Keywords: Receptor dimerization; Monte Carlo; Spatiotemporal modeling; Plasma membrane; Damköhler number; Reaction–diffusion systems; Systems biology; EGFR

1. Introduction

Extracellular signaling molecules, or ligands, bind to receptors that are either on the cell surface or within the cell. When the ligand binds a plasma membrane receptor, a signaling network is activated that relays the signal from the extracellular environment to the nucleus where the cell typically responds by a change in transcription rates. In order to tranduce the signal, the ligand bound receptors interact with a number of other proteins and lipids. For example, activation of the ErbB signaling networks leads to receptor hetero- and homodimerization and clustering; and the subsequent recruitment of other proteins, i.e., Shc, Grb2, Sos, Ras. Therefore, understanding dynamics of protein–protein interaction reactions, or bimolecular reactions, of the plasma membrane receptors along with its implications on signaling are of great importance for a wide variety of signaling pathways.

There has been a significant interest in developing predictive models to understand protein–protein interactions of signaling networks; see reviews [1–9], and most of the previous models

* Corresponding authors. Vlachos is to be contacted at Tel.: +1 302 831 2830; fax: +1 302 831 1048.
E-mail addresses: mayawala@che.udel.edu (K. Mayawala), vlachos@che.udel.edu (D.G. Vlachos), jsedwards@salud.unm.edu (J.S. Edwards).

0301-4622/$ - see front matter © 2006 Elsevier B.V. All rights reserved.
doi:10.1016/j.bpc.2006.01.008

are ordinary differential equation (ODE) models. ODE models rely on two key assumptions: (1) the system is well-mixed (spatially homogeneous, a situation also termed as global mean-field in statistical mechanics) and (2) the system is deterministic, i.e., given an initial condition, the transient evolution of the system is precisely determined [10]. For some biological processes, in particular signaling pathways, where there is a large degree of spatial organization, these assumptions may break down because every bimolecular process requires diffusion of two molecules whose collision, if successful, leads to signal propagation. Therefore, the transients of a bimolecular signaling process depend generally on the kinetic as well as the diffusive properties of the reacting proteins [2,11–13].

Partial differential equations (PDEs) are a conventional tool for incorporating the effect of diffusion in reacting systems. PDEs have been used to represent receptor–ligand dynamics [14,15] and some intracellular signaling processes [16–18]. Furthermore, the diffusion and Smoluchowski equations have been used to study diffusion-aspects of synaptic transmission [19–24]. PDEs have also been used to represent signaling processes in the plasma membrane [25–27]. Extensive research efforts have utilized PDE models for analyzing ligand–receptor interactions; see [14,15,28–41] and references therein. Similar treatments are more difficult for capturing transient receptor–receptor interactions, e.g., the bimolecular reaction between A and B can lead to different behaviors depending on the diffusivity of the higher density reactant [42]. This is because tracking the transient evolution of bimolecular reactions with reactants is, in general, a many-body problem [43]. There is a lot of research in this area; see references in [44–46]. Most of these efforts are based on the Smoluchowski [47,48] and Collins–Kimball [49] approaches. Our intent here is not to review these efforts; however, we want to point out that an exact relation between the effective reaction rate constant and diffusivity is difficult to obtain for a general two-dimensional bimolecular reaction, especially if one is interested in the transient behavior of the system. In passing, we should remark that Cahn–Hilliard and Allen–Cahn PDE formalisms, based on a free energy factional, are often used to study phase separation [50]. Finally, stochastic PDEs, such as the Langevin equation, are also used to capture the effect of noise in spatiotemporal dynamics. However, these may run in difficulties when the number of copies of proteins is small. In addition, analytical, simple solutions that could be easily used to compare to experimental data do not usually exist. A brief overview of continuum equations can be found in [51]. In this paper, we use the simplest, analytical results for the effective reaction rate constant from the standard diffusion equation (second Fick's law) [14,52] with reaction between proteins as a boundary condition (see Methods below).

Kinetic or dynamic Monte Carlo (MC) based spatial modeling is an attractive choice for modeling cell surface receptor dynamics because its computational implementation can explicitly consider (1) the creation of a spatially non-random distribution of proteins due to bimolecular reactions, (2) the spatial heterogeneity in the plasma membrane due to microdomains, and (3) the noise and the correlations resulting from a small number of copies of activated receptors. These factors are explained in detail in the next section. Another stochastic approach is based on Brownian motion (off lattice dynamics) followed by reactions [53–64]. Such studies have recently been used for bimolecular processes in the plasma membrane [65]. However, in this work we will consider only a spatial (lattice) kinetic MC model.

The importance of spatial MC modeling has recently been emphasized in several reviews [13,66,67]. Despite the existence of several spatial MC algorithms [66,68–74], the majority of MC studies have been carried out under well-mixed conditions [1,75–79]. The assumption of well-mixed condition may be justified in some biological systems, whereas for others, spatial modeling may be necessary. Currently, there is lack of a criterion which can be used to assess the need for spatial modeling for a biological system of interest, specifically bimolecular processes in the plasma membrane. Furthermore, only a few studies have emphasized the necessity of stochastic spatial modeling over deterministic spatial modeling for biological systems [66,67,69].

Herein, we assess the validity of a dimensionless number, known as the Damköhler number (Da), as a criterion to determine the importance of spatial effects of the membrane proteins on cellular signaling pathways. Furthermore, we show that the effective reaction rate changes with time due to the changes in the spatial organization of receptors. As a result, we demonstrate that the transient effective reaction rate constant of a bimolecular activation cannot be accurately captured by simple PDEs, resulting in more than one order of magnitude difference from that of MC. In biological networks, stochasticity (or noise) adds another dimension to complexity [80,81]. In the final part of this work, the effect of diffusion on noise is explored using a simple reaction network.

2. Features motivating the use of spatial MC methods

2.1. Reaction-induced spatial non-random distribution in receptor density

An initial random distribution of receptors can change into a non-random distribution due to receptor dimerization. The creation of depletion zones at steady state in receptor–receptor reactions has been discussed nicely in the past [69]. These authors showed that at steady state the effective kinetic rate constants of a PDE and a spatial MC model can differ by a factor of ~1–4. However, their study did not consider the transient variations in the distribution of receptors. Changes in distribution require a better understanding and characterization to capture the signaling receptor dynamics as well as in extracting information from experimental data.

2.2. Microenvironment heterogeneities

Recent experimental studies [82–85] suggest that understanding the dynamics and regulation of signaling pathways requires an analysis of the spatial features of the plasma membrane. Considering the advances in our knowledge about various spatial features of the plasma membrane [85–88], the

analysis of cellular signaling should include an accurate representation of the plasma membrane microdomains. In this study, we focus on the influence of plasma membrane heterogeneities on the dimerization of epidermal growth factor (EGF) receptor (EGFR). The two types of experimentally reported heterogeneities for EGFR in the plasma membrane are variations in receptor mobility [89] and in density due to localization [88,90,91]. The representation of such spatial features is easy in a spatial MC framework, especially when multiple microdomains are simultaneously considered. Also, non-random (directed) motion of receptors in the plasma membrane, as shown by [92], can be conveniently modeled using a spatial MC framework (these last two tasks are not considered in this study).

2.3. Characterization of noise

In addition to capturing transients of the activation process, the characterization of noise is important for biological signaling processes owing to the involvement of a small number of copies of signaling proteins [1,10,75,93]. Several studies have analyzed the role of stochasticity using well mixed, models (see references in [94]). However, fewer studies [36,95–98] have discussed the dependence of noise on the diffusion characteristics of a signaling network; see reviews [13,67]. Herein, using a simple signaling network, we show that diffusion can influence the noise characteristics of a signaling network.

3. Methods

3.1. Reaction systems

In the first part of this work an irreversible dimerization reaction

$$A + B \xrightarrow{k_f} AB \qquad \text{(reaction system 1)}$$

is used to understand the transient changes in the spatial organization of receptors during dimerization. Based on this understanding, in the second part of this work a reversible dimerization reaction

$$A + B \underset{k_b}{\overset{k_f}{\rightleftharpoons}} AB \qquad \text{(reaction system 2)}$$

is analyzed to assess the influence of various spatial heterogeneities of the plasma membrane. In this work, we have analyzed heterodimerization, i.e., dimerization between two different receptor types or between a ligand bound and ligand free receptor. Although, the present analysis is carried out for a heterodimerization reaction, similar concepts are also applicable to homodimerization of receptors.

Finally, to illustrate the effect of diffusion on noise, we consider a simple but more complex system than a simple dimerization reaction as shown in Fig. 1 (reaction system 3). The main reason for selecting this reaction network is its redundancy in that the ligand bound dimerized receptor can form along two reaction paths, only one of which depends on receptor diffusion. Hence, variations in diffusivity can alter the relative signaling flux between the two routes. The variation in diffusivity in the simple dimerization network only changes the time scale of the system leaving the relative concentrations of signaling proteins unchanged. This reaction network is similar to the EGF–EGFR system, as shown in [99].

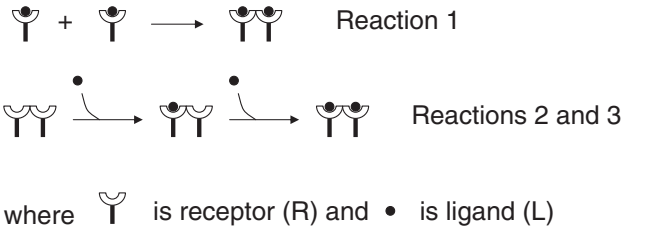

Fig. 1. Reaction network used to analyze the effect of diffusion on noise in the concentration of signaling proteins (reaction system 3). Ligand bound dimerized receptor can form either by dimerization (reaction 1) between ligand bound monomer receptors or by sequential ligand binding on predimerized receptors (reactions 2 and 3). Only the first reaction path of product formation depends on receptor diffusion.

3.2. ODE model

The ODE model entails the deterministic dynamic mass balance equations for each of the species using mass action kinetics for the forward and backward (if one is included) reactions. The following equation represents the dynamic mass balance corresponding to reaction system 1

$$-\frac{d\theta_A}{dt} = k_f \theta_A \theta_B, \qquad (1)$$

where t is time, θ represents the number of receptors per site or fraction of occupied lattice sites by each receptor, and k_f is the macroscopic reaction rate constant with units of [(receptors/site)$^{-1}$ s^{-1}]. The ODE model is solved using MATLAB.

3.3. PDE models

In this work, the effective kinetic rate constants obtained from a steady state [14] and a transient [52] PDE (the simple diffusion equation) have been used in an ODE model to track the transient evolution of proteins. We leave more complicated analytical treatments, such as those in [44], mainly because they are unavailable for complex systems involving hundreds of proteins in signaling networks [100]. These earlier PDE based approaches consider dimerization in 2D and assume diffusion of molecules B towards stationary molecules A with a diffusivity that is the sum of the diffusivities of A and B (see references in [69]). Lauffenburger and Linderman [14] derived an expression for the effective kinetic rate constant (k_{PDE}) given as

$$k_{PDE} = \frac{2\pi D_{AB} k_{Areal}}{2\pi D_{AB} + k_{Areal}\ln(b/s)} = \frac{4\pi D_{AB} k_{Areal}}{4\pi D_{AB} + k_{Areal}\ln(1/\pi\rho_A s^2)}, \qquad (2)$$

Table 1
List of microscopic events and expressions to calculate the transition rates

Microscopic event	Transition rate
Diffusion	$\Gamma^{\mathrm{d}}_{i\to j}=\frac{1}{4}\Gamma^{\mathrm{d}}\sigma_i(1-\sigma_j), j\in B_i,$ – σ_i is the occupancy (discrete) function that is 1, if site i is filled, and 0, if site i is empty (a single index indicating the site is used to simplify notation). – $\Gamma^{\mathrm{d}}=\frac{D}{a^2}$, where a is the microscopic lattice pixel dimension taken equal to the encounter radius ($a=s=2$ nm, i.e., the pixel dimensions of the microscopic lattice are set such that receptors that are first nearest neighbors can react), and D is the diffusivity of a receptor. – B_i denotes the set of sites to which diffusion from site i can occur. In our model, this set includes all 4 first-nearest neighboring sites.
Dimerization reaction ($A+B\to AB$)	$\Gamma^{\mathrm{r}}_{i\to j}=\frac{k_{\mathrm{f}}}{4}\sigma_i\sigma_j$ – k_{f} is the macroscopic reaction rate constant with units as [(receptors/site)$^{-1}$ s^{-1}].
Decomposition reaction ($AB\to A+B$)	$\Gamma^{\mathrm{r}}_i=k_{\mathrm{b}}\sigma_i$ – k_{b} is the macroscopic reaction rate constant with units as [s^{-1}].

where $D_{AB}=D_A+D_B$, D_A and D_B are the diffusivities of A and B, respectively, ρ_A is the density of molecules of A (number of molecules per unit area), $b=\sqrt{1/\pi\rho_A}$ is one-half of the mean distance between molecules of A distributed in a certain area, k_{Areal} is the intrinsic reaction rate constant in units of (receptors/area)$^{-1}$ s^{-1}, and s ($s=2$ nm in this work) is the encounter radius. k_{Areal} and k [(receptors/site)$^{-1}$ s^{-1}], used in the hybrid null-event MC algorithm discussed below, are related using the encounter radius (see Table 1), as follows

$$k_{\mathrm{Areal}}=ks^2. \tag{3}$$

The diffusion-limited reaction rate constant, $k_{\mathrm{Diffusion}}$, can be extracted from Eq. (2) by comparing it with the following expression [14] based on the resistance in series model

$$k_{\mathrm{PDE}}=\left(\frac{1}{k_{\mathrm{Areal}}}+\frac{1}{k_{\mathrm{Diffusion}}}\right)^{-1} \tag{4}$$

yielding

$$k_{\mathrm{Diffusion}}=\frac{4\pi D_{AB}}{\ln(1/\pi\rho_A s^2)}. \tag{5}$$

Note that Eq. (2) has been derived by solving the quasi-steady state diffusion equation. However, as time progresses, b varies because the number of molecules of A, and hence ρ_A, decreases due to reaction.

Torney and McConnell [52] considered a transient model and derived the following expression for the diffusion-limited case at long times

$$k_{\mathrm{Diffusion}}\sim\frac{4\pi D_{AB}}{\ln(4D_{AB}t/s^2)-1.2}. \tag{6}$$

By analogy with Eq. (4), the effective reaction rate constant can be approximated using the resistances in series model

$$k_{\mathrm{PDE}}=\frac{4\pi D_{AB}k_{\mathrm{Areal}}}{4\pi D_{AB}+k_{\mathrm{Areal}}[\ln(4D_{AB}t/s^2)-1.2]}. \tag{7}$$

As a note, Eq. (7) cannot be used at short times, $t\le t^*$ ($t^*=0.83s^2/D_{AB}$) because $k_{\mathrm{Diffusion}}$ becomes negative. This occurs because Eq. (6) is an approximate expression derived by neglecting some terms [52]. Using the expression of k_{PDE} (Eqs. (2) or (7)) in an ODE model, the time evolution of the system can be traced, e.g., for the reaction system 1, k_{PDE} is used in place of k_{f} in Eq. (1).

These PDE models assume that the diffusion fields of individual receptors do not overlap, i.e., the distribution of receptors around each sink is not influenced by the presence of other sinks. This assumption is valid only for sufficiently low densities of receptors. An additional assumption in the approach of Lauffenburger and Linderman [14] is the quasi-steady state. These assumptions may cause deviations when used for the calculation of the rate constant under transient conditions. Additionally, unequal densities of dimerizing species are not considered in Eqs. (2) and (7) and may lead to difficulties, such as the calculation of 'b' in Eq. (2). Finally, continuum models do not account for the discrete representation of receptors. However, as shown below, PDE based models can be used to get an order of magnitude estimation of the effective reaction rate constant.

3.4. Hybrid null-event MC algorithm

The spatial MC simulations were performed by implementing a hybrid null-event MC algorithm using FORTRAN 90. The algorithm uses an efficient selection strategy by picking occupied sites only, and an easily programmable null-event MC algorithm [71]. The algorithm is briefly explained below; for details see [71].

The spatial domain is represented using a 2D square lattice. The lattice is initially randomly populated with a given density of receptors. Periodic boundary conditions are employed, which are adequate for the entire plasma membrane [101]. After initialization, an occupied site is randomly picked and one of the microscopic events (diffusion, forward or backward reaction) is selected to possibly occur, based on probabilities calculated below.

Table 1 lists the transition rates, Γ^x_i, of all the microscopic events in our simple dimerization reaction system at a selected site i, where 'x' denotes an event (reaction, 'r' or diffusion, 'd'). The probability, p^x_i, for a certain event is calculated as

$$p^x_i=\frac{\Gamma^x_i}{\Gamma_{\max}}, \tag{8}$$

where $\Gamma_{\max}$ is a normalization constant. One convenient way to define the normalization constant is

$$\Gamma_{\max}=\Gamma^{\mathrm{d}}+\max\left\{\sum_{\text{all reaction events}}\Gamma^{\mathrm{r}}\right\}. \tag{9}$$

For our simple model with only one dimerization reaction,

$$\Gamma_{\max} = \Gamma^{\mathrm{d}} + k_{\mathrm{f}} + k_{\mathrm{b}}, \tag{10}$$

where subscripts f and b refer to the forward and backward reaction events, respectively. A random number 'ζ' is finally chosen from a uniform distribution between 0 and 1. The events are randomly ranked. The smallest value of m satisfying the following criterion is chosen

$$\sum_{x=1}^{m} p_i^x > \zeta. \tag{11}$$

If there is no value of m satisfying the above criterion, then no event is selected to occur (a null-event) and a new occupied site is again randomly picked. Otherwise, the m^{th} event is selected, the populations on the lattice are updated accordingly to reflect the reaction or diffusion process, and the real time is advanced as suggested by [71]. In our simulations, the real time is advanced based on the diffusion of receptors according to which the average time step after each successful diffusion event is calculated as (for notation see Table 1)

$$\Delta t = \frac{1}{\frac{1}{4}\Gamma^{\mathrm{d}} \sum\limits_{\text{occupied sites}}} \left(\sum_{j \in B_i} (1-\sigma_j) \right). \tag{12}$$

The independence of results on lattice size is shown in the Appendix.

3.5. Calculation of effective kinetic rate constant from MC simulations

The slope of the coverage (θ_i=Sites occupied by i^{th} species/Total sites)–time profile of the reactant (A or B) obtained from the spatial MC simulations was used to calculate the effective rate as follows

$$k_{\mathrm{SpatialMC}} = -\frac{\mathrm{Slope}}{\theta_A \theta_B}. \tag{13}$$

The coverage–time profile used is the mean of a given number of simulations that is mentioned in the figure captions.

3.6. Effectiveness factor

The effectiveness factor shows the reduction of the actual reaction rate of a spatial model due to the effect of diffusion. Since in a well-mixed system there are no diffusion limitations, the reaction rate in the well-mixed model is the maximum reaction rate. Thus, the deviation of the rate of a spatial model from that of the ODE-based model provides a convenient way to compute the effectiveness factor

$$\eta = \frac{\text{Reaction rate from spatial model}}{\text{Reaction rate from well} - \text{mixed model}}. \tag{14}$$

In this work, the reaction rate in the denominator is easily calculated as $k_f \theta_A \theta_B$, using the global mean-field approximation.

3.7. Damköhler number (Da)

The effectiveness factor is calculated at different times for several values of the intrinsic reaction rate constant (k) and diffusivity (D). The various combinations of k and D can be summarized in terms of a dimensionless number, known as the second Da number, which is traditionally defined as the ratio of the time scales of diffusion and reaction [102]. For the dimerization reaction, we have defined the second Da number (we have dropped the prefix 'second' for simplicity in later discussions) in a modified way as the ratio of the time scales of collision and reaction events. The collision time, instead of diffusion time, not only considers the time scale for jumping from one site to the next but also the density of receptors. For a dimerization reaction event to happen, the two reacting receptors should first collide, i.e., brought in contact by diffusion, and then react. As the density of receptors decreases, the average distance between receptors increases and so does the time for collision. Essentially, the Da number compares the time needed to bring together the reacting species (for collision) and the time needed for reaction after they collide.

Calculation of the Da number requires knowledge of the distribution of distances between receptors at each instance, a task demanding a spatial MC simulation. In order to make this a simple and useful criterion, the global mean-field approximation has been invoked in estimating the Da number. This assumption makes the computation of Da number possible using macroscopically available parameters, such as the reaction rate constant and diffusivity. In the limit of low concentration, the areal collision rate, $\Gamma^{\mathrm{Areal}}_{\mathrm{MF\text{-}collision}}$, i.e., the number of collisions per unit time per unit area, is given by [52]

$$\Gamma^{\mathrm{Areal}}_{\mathrm{MF-collision}} = 4 D_{AB} \rho_A \rho_B, \tag{15}$$

where ρ_A and ρ_B are areal number densities (number of receptors per unit area) of A and B, and D_{AB} is sum of the diffusivities of A and B. By introducing the coverage, θ, of each species, Eq. (15) can be written as

$$\Gamma_{\mathrm{MF-collision}} = \left(\frac{4 D_{AB}}{s^2} \right) \theta_A \theta_B = \Gamma^{\mathrm{d}}_{AB} \theta_A \theta_B, \tag{16}$$

where $\Gamma^{\mathrm{d}}_{AB} = 4 D_{AB}/s^2$ is the total transition rate of diffusion in all four directions on the square lattice and the rate of collision, $\Gamma_{\mathrm{MF\text{-}collision}}$, is calculated per unit site. In the well-mixed model, diffusion is assumed to be infinitely fast. Thus, the dimerization rate is purely controlled by the intrinsic speed of the chemistry, k_{f}, and the coverages of receptors as written below

$$\Gamma^{\mathrm{r}}_{\mathrm{MF-ODE}} = k_{\mathrm{f}} \theta_A \theta_B. \tag{17}$$

The units of $\Gamma^{\mathrm{r}}_{\mathrm{MF\text{-}ODE}}$ are number of reaction events per unit time per lattice site.

Since Eqs. (16) and (17) show the same functional form, the ratio of time scales is independent of the coverage and can be written as

$$\mathrm{Da} = \frac{\text{Time scale of collision event}}{\text{Time scale of reaction event}} = \frac{\Gamma^{\mathrm{r}}_{\mathrm{MF-ODE}}}{\Gamma_{\mathrm{MF-collision}}} = \frac{k_{\mathrm{f}}}{\Gamma^{\mathrm{d}}_{AB}} = \frac{k_{\mathrm{f}} s^2}{4D_{AB}} = \frac{k_{\mathrm{f,Areal}}}{4D_{AB}}. \quad (18)$$

4. Results and discussion

4.1. Reaction-induced spatial correlations in receptor density

4.1.1. Comparison of spatial MC with continuum (ODEs and PDEs) models

Fig. 2 compares the transient coverage profiles of A ($=B$) during the irreversible dimerization reaction (reaction system 1) obtained using ODE, PDEs (Eqs. (2) and (7)), and spatial MC models for an initial coverage of $\theta_{A_o}=\theta_{B_o}=0.2$ and $Da=25$. The curve corresponding to the transient model of [52] starts at time t^* because $k_{\mathrm{Diffusion}}$ becomes negative for $t<t^*$, as explained earlier in the Methods section. The coverage of A decays faster in the ODE model because of the lack of diffusion limitations. The difference between the ODE and the spatial models (in particular the spatial MC model) is less at very short times; however, it becomes more profound as reaction progresses. The PDE models also differ from the spatial MC model. Interestingly, the initial rate of decay of A is faster in the spatial MC as compared to the PDE model; however, the differences are not as dramatic at longer times.

These observations indicate that the effect of diffusion on reaction rate varies possibly with time. To further understand the effect of diffusion, we computed the effectiveness factor, a quantity that is more related to signaling, using our spatial MC model. Fig. 3 shows the transient effectiveness factor as a function of coverage (note that decreasing coverage corresponds to increasing time) for three different initial densities of A and B and four values of the Da number in the range of 0.025–25. A sufficiently small Da number (e.g., $Da=0.025$) indicates that diffusion is fast; as a result, an ODE model may be adequate to compute the effective reaction rate (when stochasticity may be neglected). Fig. 3 shows that diffusion limitations can significantly affect the effective signaling rate (see curves corresponding to $Da \geq 0.25$). An important point to

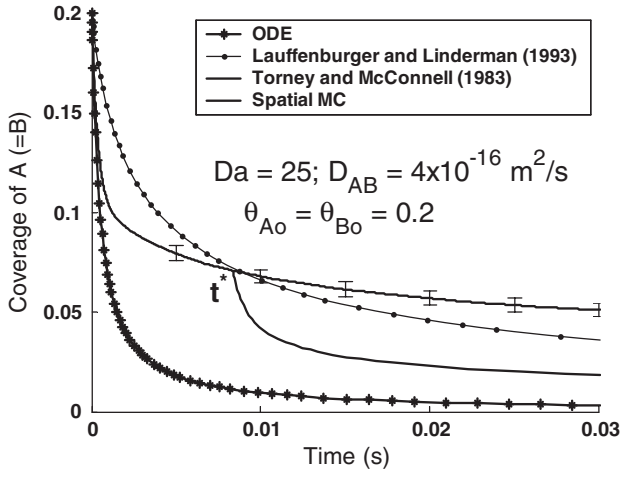

Fig. 2. Comparison of transient coverage profiles of A ($=B$) for $Da=25$ obtained using various models. The curve corresponding to the transient model of Torney and McConnell starts later due to the limitation of Eq. (7) that yields negative values at short times, $t \leq t^*$.

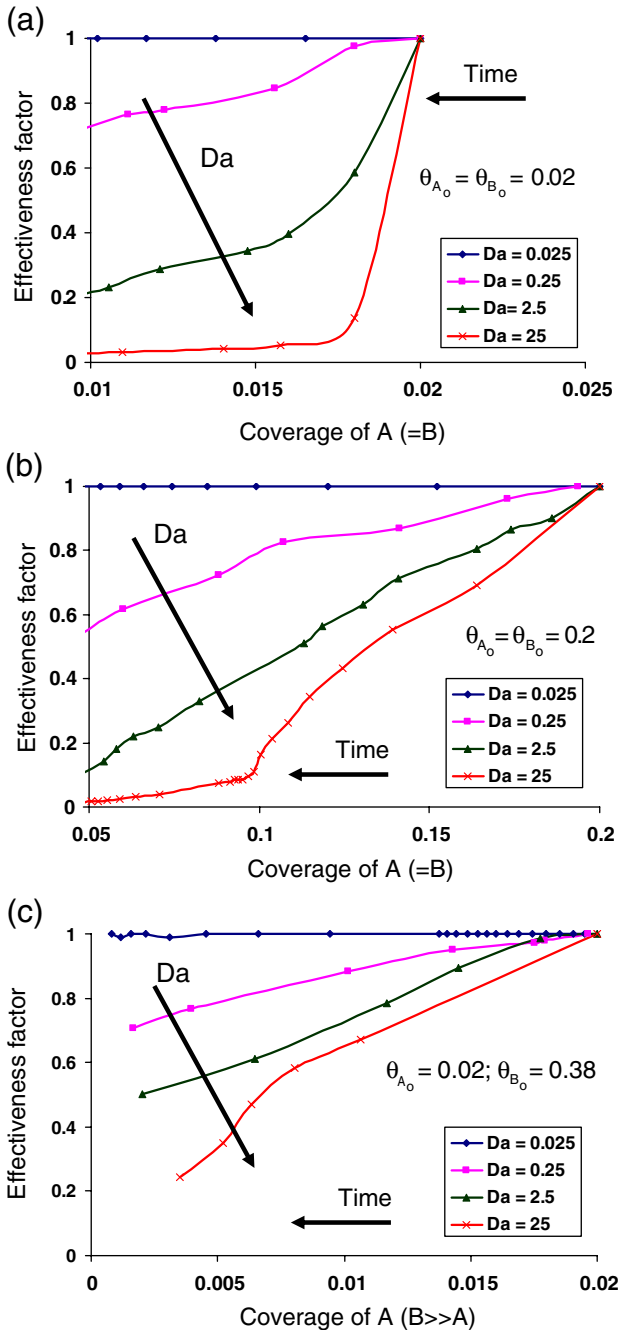

Fig. 3. Variations in effectiveness factor with time (coverage) for different values of Da number in the range 0.025–25 for three different initial receptor coverages (subscript o denotes initial conditions): 0.002, 0.02, 0.2. Curves represent mean and error bars represent 2 standard deviations of 30 simulations with different random number seeds.

realize from the transient effectiveness factor curves is that the effect of diffusion on reaction rate becomes more profound as time progresses. Based on Fig. 3, spatial modeling is needed for $Da > \sim 0.1$. We tested this criterion over a wide range of densities of 100–100,000 receptors/μm^2, i.e., $\theta = 0.0004$–0.4 (comparisons at lower densities are not shown), which are representative of the density of many types of receptors in the plasma membrane.

The results of Fig. 3 underscore the relevant time scales requiring spatial modeling. In order to assess how well PDE models can describe spatial features, Fig. 4(a) and (b) compare the spatial MC dimerization rate constant with the two PDE-based rate constants. The three regions in each figure compare the effective rate constant for a fixed value of *Da* number (2.5 and 25 in Fig. 4(a) and (b), respectively) corresponding to three initial coverage values (0.002, 0.02, 0.2). These simulations start at $t = 0$ with a spatially random distribution of receptors; a decrease in coverage represents time evolution. While the differences in coverages shown in Fig. 2 between various models are not dramatic, there is profound difference in effective rate constants between the spatial MC and PDE models. In particular, the quasi-steady state model of [14] follows a continuous response that is independent of initial coverage. On the other hand, the other models show a family of solutions that depend on the initial coverage (spatial MC) or time elapsed (transient model). Deviations up to two orders of magnitude between the spatial MC and the PDE models are observed. The deviations in Fig. 4 are due to the transient variations in the distribution of the receptors that are not accounted for by the PDE models. These variations are explored in detail in the next section.

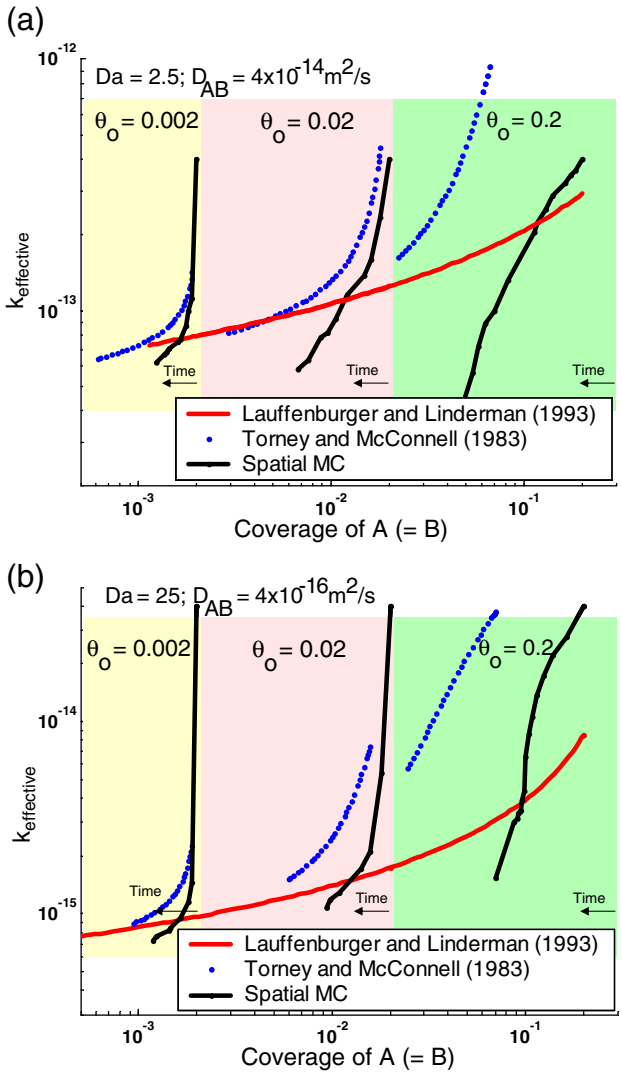

Fig. 4. Comparison of effective rate constant, obtained using the spatial MC and PDE models, vs. time for three different initial coverage (0.002, 0.02, 0.2) of *A* (=*B*) and *Da* number of (a) 2.5 and (b) 25. Curves represent the mean of 30 concentration profiles obtained using different random number seeds.

Our simulations suggest that PDE models perform worse at higher receptor densities. At first, this observation seems counterintuitive because higher receptor density suggests short distances to diffuse rendering spatial effects less important. However, at higher receptor densities the assumption of non-overlapping diffusion fields breaks down. The transient model of [52] behaves well at short times for sufficiently dilute systems but deviations are observed at longer times due to spatial correlations encountered in the MC model.

An interesting observation from the simulation results is that for the same *k*, *D* and instantaneous coverage, different effective kinetic constants can be deduced (at different time instants) depending on the initial coverage of the receptors (Fig. 4(a) and (b)). The dependence of effective kinetic rate constant on time and initial coverage can have two important implications with respect to: (1) biological control and (2) estimation of the dimerization rate constant from experiments. The simulations show that the effective transient signaling rate constant depends on the initial local density of the receptors. Experimental studies have suggested localization of receptors in various microdomains in the plasma membrane [103]. Our simulations show that localization can help in maintaining a high effective dimerization rate constant, as shown in Fig. 3. The decay of effective reaction rate constant with coverage (time) at lower local density (Fig. 3(a)) occurs faster than at higher receptor density (Fig. 3(b) and (c)). This dependence is briefly discussed later in Section 4.3. The decrease of the effective kinetic rate constant with time (at lower density during later phases of dimerization) may also help in suppression of low, noisy signals which can develop in late phases of signaling.

The above discussed observation has important implications for understanding experimental data involving interpretation of receptor dimerization following an extracellular signal, e.g., ligand binding. To obtain the dimerization rate constant from experiments, one should keep in mind that the effective dimerization rate constant changes with time (or density of receptors). Therefore, estimation of kinetic parameters from the experimental data should not be done based only on an instantaneous average receptor density. Instead, a spatial MC model, based on the initial receptor density, diffusion constant and time after stimulation should be considered in data interpretation. Future studies will explore these issues.

4.1.2. Spatially non-random distribution of receptors during dimerization

Fickian diffusion of receptors leads to an environment where the receptors are distributed randomly. On the contrary, bimolecular reactions, e.g., dimerization, consume monomer receptors creating regions that have a low number of monomer receptors in the plasma membrane. As a result, there are local depletion zones [69]. These two mechanisms work in opposition. The relative speeds of diffusion and intrinsic reaction dictate whether or not the receptors are distributed randomly. To understand the spatial distribution of receptors in the presence of a dimerization reaction, we simulated the prototype, irreversible dimerization reaction between A and B (reaction system 1) for different initial coverages of A and B and various values of reaction rate constants and diffusivities.

We used the product $\theta_A\theta_{B/A}$ as a measure of the spatial correlations of the receptors, where $\theta_{B/A}$ is the conditional probability of having a first-nearest neighboring site occupied by B given that the central site is occupied by A. Specifically, it is

$$\theta_{B/A} = \frac{N(1,t)_{B\to A}}{\text{Total sites around free } A \text{ at the first} - \text{nearest neighbor location}}, \quad (19)$$

where at a particular time, t, $N(1,t)_{B\to A}$ is the total number of free (not dimerized) molecules of B at the first nearest neighbor location around all free molecules of A. For a square lattice, the denominator is 4 times the total number of free molecules of A.

If surface diffusion is Fickian and fast enough to homogenize the receptors, then the occupation of a site by receptor B is independent of A, giving $\theta_A\theta_{B/A}=\theta_A\theta_B$ [104]. Under such conditions, the dynamics can be described using the ODE model. Fig. 5 compares MC results for $\theta_A\theta_{B/A}$ vs. $\theta_A\theta_{B/A}$ for three different initial densities of A and B and four values of the Da number in the range of 0.025–25. In Fig. 5, the reduction in coverage implies time evolution.

In our simulations, receptors are initially randomly distributed on the plasma membrane. Such a distribution results in some AB pairs in close proximity at $t=0$ depending on the receptor density (this may not be true at very low receptor densities). Consequently, all curves start from the top-right corner of Fig. 5, close to the $\theta_A\theta_{B/A}=\theta_A\theta_B$ line. The resemblance of Figs. 3 and 5 indicates that the reduction in the effectiveness factor with increasing time is due to changes in the distribution of receptors.

For low values of the Da number, such as 0.025 (at the receptor densities shown in Fig. 5), $\theta_A\theta_{B/A}$ is equal to $\theta_A\theta_B$, representing lack of correlations at all times as a result of diffusion being sufficiently fast in comparison to reaction. Therefore, the corresponding curve in Fig. 3 shows that the effectiveness factor is 1 during the transient dimerization process.

An increase in the Da number means a decrease in the time scale of reaction (a higher kinetic rate constant) and/or an increase in the time scale of collisions (a lower diffusivity). This leads to inability of diffusion to homogenize the system at the fast rate of reaction. The result is spatial correlations as

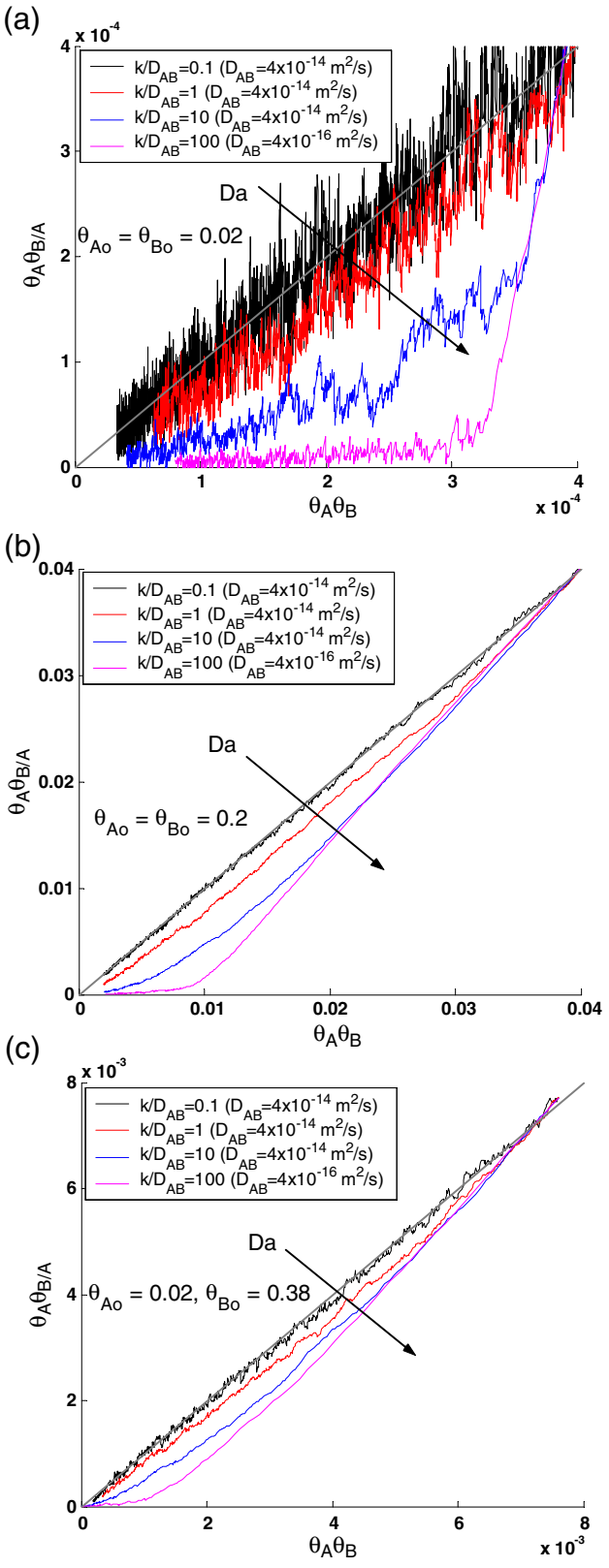

Fig. 5. Variations in $\theta_A\theta_{B/A}$ with time as a function of $\theta_A\theta_B$ for different values of Da number in the range 0.025–25 and three different initial receptor coverages (subscript o denotes initial conditions): 0.002, 0.02, 0.2. Curves represent the mean of 30 simulations with different random number seeds. The gray dashed diagonal line represents $\theta_A\theta_{B/A}=\theta_A\theta_B$.

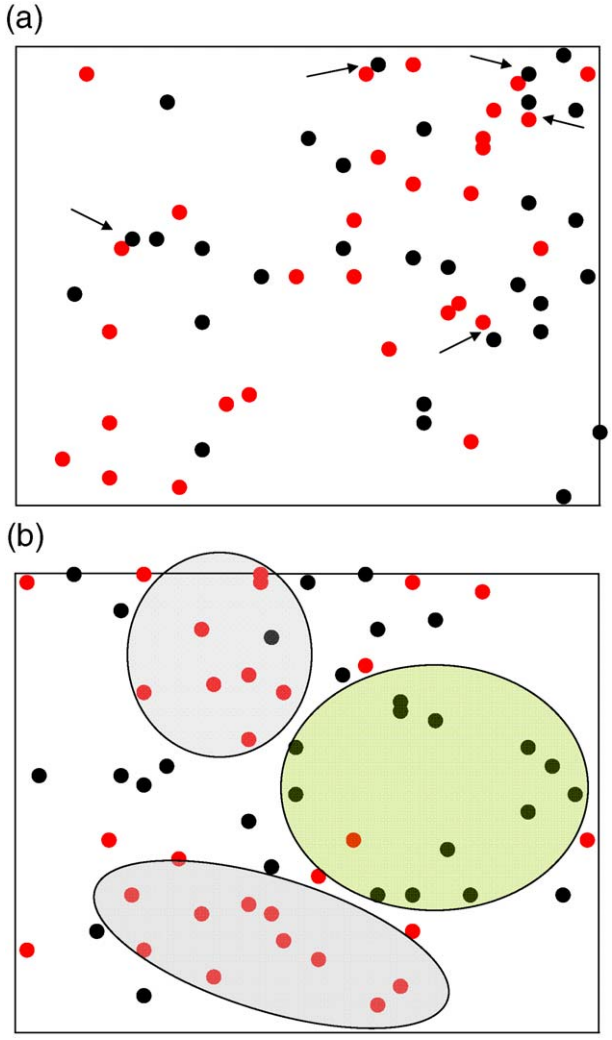

Fig. 6. Snapshots of receptor distribution corresponding to Fig. 5(a) for (a) $Da=0.025$ and (b) $Da=25$ taken after 40% of the receptors have been consumed. Only monomer receptors are shown, each type in a different color. The arrows in (a) show receptors in close proximity for reaction. The colored oval shaped regions in (b) show areas enriched with one receptor.

discussed recently by one of us [104]. Therefore, in Fig. 5 an increase in the Da number leads to an increased deviation of the $\theta_A\theta_{B/A}$ curve from the diagonal $\theta_A\theta_{B/A}=\theta_A\theta_B$ line. The decrease in $\theta_A\theta_{B/A}$ occurs at a smaller rate when the initial densities of A and B are high (Fig. 5(b)) and is the least when one of the receptors is in excess (Fig. 5(c)) because of the presence of more AB pairs at $t=0$.

Snapshots of receptor distribution are shown in Fig. 6. The two plots correspond to Fig. 5(a) for $Da=0.025$ and $Da=25$. Fig. 6(a) shows random distribution with some pairs of A and B. In contrast, Fig. 6(b) shows regions enriched with one receptor type.

Fig. 7 further characterizes the transient changes in the spatial distribution of receptors at a particular value of $Da=2.5$. The horizontal axis represents the coverage that decreases with time from right to left as dimerization proceeds. The vertical axis is the normalized probability for finding B at the i^{th} nearest neighbor location around A. The normalized probability represents the local receptor coverage normalized by the global receptor coverage. Similar to [105], the normalized probability is calculated as

$$\text{Normalized probability}(i,t)=\frac{\left(\frac{N(i,t)_{B\to A}}{N(i,t)_A}\right)}{\theta_B}, \tag{20}$$

where at a particular time, t, $N(i,t)_{B\to A}$ is the total number of free molecules of B at the i^{th} nearest neighbor location around all free molecules of A, $N(i,t)_A$ is the total number of sites at the i^{th} nearest neighbor location around all free molecules of A (which for our square lattice is 4 times the total number of free molecules of A). For a random distribution, the normalized probability is 1 independent of location and time (horizontal dashed line). The two curves in Fig. 7 correspond to the normalized probability of the first and the eighth nearest neighbor locations as a function of decreasing coverage as dimerization proceeds. The curves show that dimerization produces local spatial correlations by creating depletion zones. The depletion zones represent regions where the local coverage (first nearest neighbor curve) decreases at a faster rate as compared to the decreases in the total coverage (eighth nearest neighbor curve). The depletion zones lead to a lower dimerization rate in the spatial MC model as compared to the rate of the ODE model (which depends on the total coverage). These results are consistent with Fig. 6.

4.2. Effect of plasma membrane spatial features on the dimerization rates

We have shown that the effective kinetic rate constant depends on the diffusivity and initial density of receptors. These two features have been reported to vary in different parts of the plasma membrane. To study the effect of plasma membrane spatial features, we consider a reversible reaction between A and

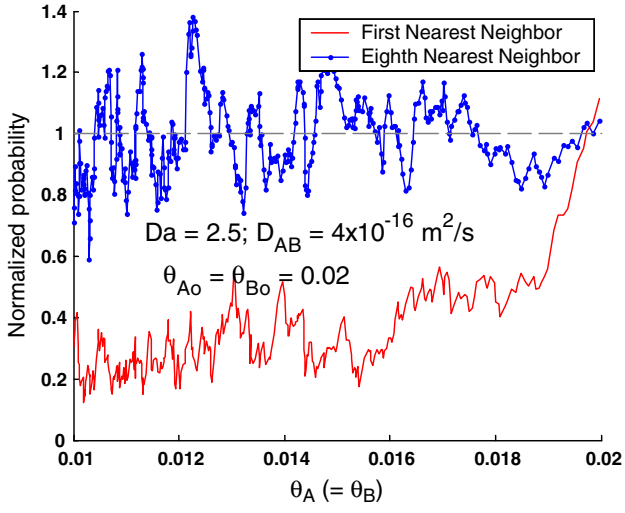

Fig. 7. Normalized probabilities (see text) at first and eighth nearest neighbor locations vs. coverage for equal initial coverage of 0.02; $Da=2.5$ and $D_{AB}=4\times10^{-14}$ m^2/s. Deviations of the probability from 1 indicate the formation depletion zones at short distances. Time dependent deviations show the transient nature of receptor distribution. Curves represent the mean of 30 concentration profiles obtained using different random number seeds.

B representing EGFR dimerization, as shown in reaction system 2. The intrinsic kinetics of EGFR dimerization is taken in the range $1–10^2$ without ligand and $10^3–10^4$ $(\text{molecules/site})^{-1}\,\text{s}^{-1}$ when the receptor is bound to ligand [99]. The equilibrium constant is taken as 8×10^{-3} $(\text{molecules/site})^{-1}$ [99]. This value is kept fixed to enable comparison of the transient reaction rate with the same equilibrium concentrations. For this section, the effectiveness factor is computed as the ratio of the net forward rate of the spatial MC model over that of the ODE-based model at 33% of the equilibrium dimer concentration (representing the initial phase of dimerization process). Fig. 8 shows the effectiveness factor vs. *Da* number for three initial receptor densities, indicated in the legend. This graph allows to study the effect of variations in receptor density and mobility on signaling. Three heterogeneities, described below, are analyzed in this study.

4.2.1. Variations in receptor density due to cell type

We performed simulations with various receptor expression levels that correspond to different cell lines ranging from overexpression, such as A-431 cells with $\sim2\times10^6$ EGFR [106] and HER82 [107] to normal expression $\sim4\times10^4–2\times10^5$ receptors/cell of EGFR, such as COS, B82, HeLa, NIH-3T3: HER84, HER22, MCF7 and human glioma cells.

In our simulations, the lowest receptor density of 100 EGFR/μm^2 (50 molecules of *A* and 50 molecules *B* on a 1000×1000 nm lattice) represents EGFR expression in normal cells. The next density level of 10,000 receptors/μm^2 (50 molecules of *A* and 50 molecules *B* on a 100×100 nm lattice) corresponds to cells that overexpress EGFR, such as A-431 cells. These two cases span the range of EGFR density in most of the cell types.

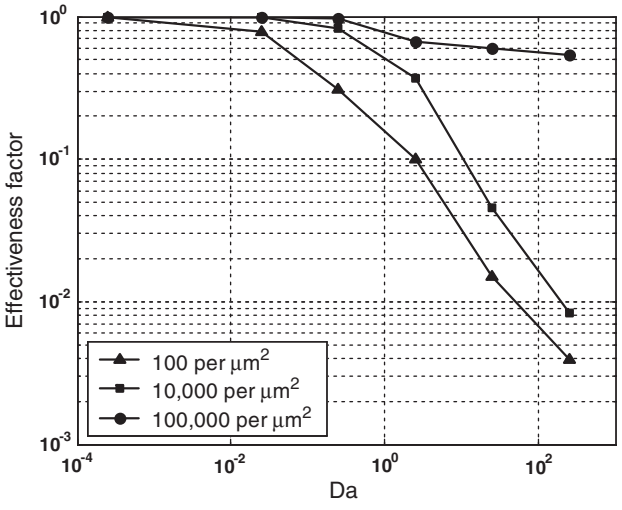

Fig. 8. Effectiveness factor as a function of *Da* number calculated at 33% of the equilibrium concentration of the dimer produced from the reversible dimerization reaction between *A* and *B*. The densities reported on the plot are the initial densities. The bottom curve is representative of an average EGF receptor density in typical normal cells, the middle curve of localization in normal cells and of an average EGF receptor density in cancer cells, and the top curve of localization in cancer cells. The points represent the mean of 30 concentration profiles obtained using different random number seeds and the lines just connect the points.

In addition, the plasma membrane expressions of several other types of receptors, such as the G-protein coupled receptors (GPCR), are also in similar ranges [105].

4.2.2. Variations in receptor density due to localization

Over the past decade, there have been studies that suggest microdomains within the plasma membrane can play an important role in cell signaling [86,87,91,108–111]. One of the key spatial features of the membrane microdomains is that proteins are often localized to these microdomains. Several studies have indicated that EGFR localizes in lipid rafts or cholesterol-rich microdomains of the plasma membrane [91,103]. The receptors and proteins localized microdomains in the plasma membrane have been proposed to act as signaling platforms [91,103]. Therefore, the role of localization in biological membranes is an issue of high interest for understanding the cellular signaling. Further support of this hypothesis comes from our recent study that shows an influence of localization of EGFR within the plasma membrane on EGF–EGFR binding characteristics [112].

4.2.3. Variations in receptor mobility

The diffusivity of EGFR has been reported in the range of $10^{-9}–10^{-13}$ cm^2/s by [113]. Recently, it has been suggested that this range is likely due to association with cytoskeletal membrane corals [114] or lipid rafts [115].

4.2.4. Effect spatial heterogeneity on the EGFR dimerization rate

As expected, the lowest effectiveness factor is observed for the dimerization of ligand bound receptors in the plasma membrane microdomains with reduced mobility (i.e., large *Da* number in Fig. 8). In cell lines with a normal density of EGFR, diffusion limitations can significantly lower the dimerization rate by over 2 orders of magnitude (bottom curve in Fig. 8). Such a significant decrease is also observed for cell lines with higher EGFR expression, such as human A-431 epidermoid carcinoma cells (middle curve in Fig. 8). To represent localization of EGFR on A-431 cells, we simulated a density of 100,000 receptors/μm^2 (500 molecules of *A* and 500 molecules *B* on a 50×50 lattice).

For normal cells, even a 100 fold higher density causes only $\sim$2–3 fold increase in the diffusion limited dimerization rates, as shown in Fig. 8, in which a wide range of *Da* numbers is considered (compare bottom and middle curves in Fig. 8). This shows that localization is unlikely to cause a significant increase in diffusion limited EGFR dimerization rates in normal cells, which is in line with the suggestions of Kholodenko [116] for intracellular localization. However, in A-431 cells, only a 10 fold higher density leads to 1–2 orders of magnitude increase in the dimerization rate (middle and top curves in Fig. 8). This shows that in A-431 cells, the dimerization rate is greatly enhanced due to localization. Hence, the fraction of EGFR localized on A-431 cells can lead to significantly faster signal propagation. However, analysis of a detailed signaling pathway will be required to understand the biological implication of this observation, and will be the focus of future studies.

Fig. 8 shows a significant influence of biophysical characteristics over the effective dimerization dynamics providing a level of control over almost inflexible kinetic parameters. The plasma membrane microdomains can influence the signaling events in two ways: (1) local receptor mobility and (2) local receptor concentration. The spatial characteristics can alter the bimolecular reaction rates in the plasma membrane by up to two orders of magnitude in the initial phases of reaction.

4.3. Effect of receptor diffusion on concentration fluctuations

The effect of kinetic parameters on noise has been explored using a well-mixed model [78]. As shown above, the effective kinetic rate constant depends on diffusivity for $Da > \sim 0.1$. The noise characteristics of a system are also known to depend on the number of copies of reacting species [78,81,117,118]. Diffusion can play a significant role in controlling the effective reaction rate constant and the transient number of copies of various signaling proteins. Hence, diffusion could influence the fluctuations in concentration.

In order to explore this issue, we simulate the reaction system 3, shown in Fig. 1. We assume the first reaction to occur with fast intrinsic kinetics ($k = 10^5$ site s^{-1}). The ligand binding reactions are simulated with $k_L = 100\ s^{-1}$, assuming a constant ligand (L) concentration. The reaction network is simulated for two values of diffusivities: $D = 2 \times 10^{-13}$ m^2/s and $D = 2 \times 10^{-16}$ m^2/s [113]. Initially, 40 ligand free dimers (R_2) and 100 ligand bound monomers (RL) are randomly placed on a 100×100 nm lattice. To estimate the noise in the concentration of $(RL)_2$, the standard deviation of its concentration is calculated based on 9000 simulations with different random number seeds. Fig. 9 shows the noise in the concentration of $(RL)_2$ as a function of its concentration for the same kinetic parameters but two different diffusivities.

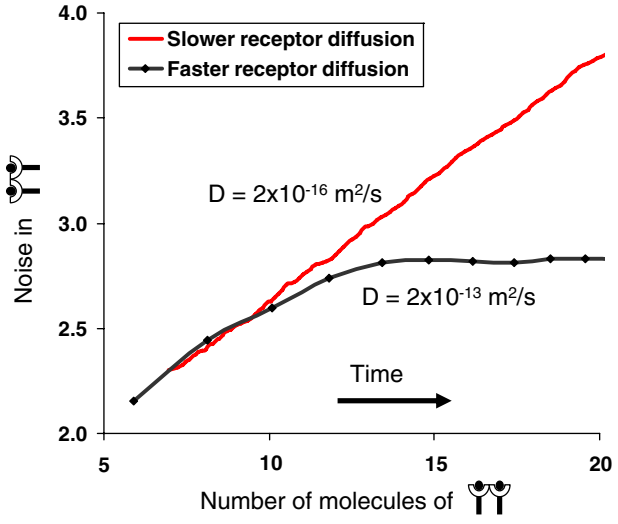

Fig. 9. Noise in the concentration of ligand bound dimerized receptor plotted as a function of its concentration. The signaling network is shown in Fig. 1. Both profiles were obtained for the same kinetic parameters but different values of diffusivities for monomer receptor diffusion. The data for this figure is obtained from 9000 runs using different random number seeds.

To understand the observed noise characteristics, we analyze the concentration profiles of the individual proteins. The noise characteristics of a network depend on the absolute as well as the relative number of copies of the signaling proteins. Therefore, the dynamic concentration profiles of various proteins in a multicomponent system determine the transient noise characteristics. When diffusion is fast, almost all of the initial $(RL)_2$ forms via the first reaction and reactions 2 and 3 play a negligible role. In contrast, when diffusion is slow, the contributions of reactions 2 and 3 to the initial $(RL)_2$ formation are substantial. The different transient composition (in terms of the number of copies of chemical species) leads to differences in noise characteristics.

Redundancy is a common characteristic of biological networks [119]. The overall signaling network consists of many reactions which provide alternate routes to the same final biological product. Past studies have reported redundancy as a mechanism to attenuate the effect of noise in non-spatial models [10,120,121]. Herein, we show that diffusion can influence the relative information flow through different pathways, and therefore can play an important role in determining the transient noise characteristics. Thus, the different functional dependence of redundant signaling pathways on biophysical characteristics, such as diffusivity, provides a means of exerting control on not only the information (or material) flow but also on the noise characteristics associated with the flow.

5. Conclusions

In the first part of this work, we studied reaction-induced spatial correlations in receptor density. We compared ODE, simple PDEs and spatial MC models using simple dimerization reaction systems in terms of transient concentration profiles and transient effective reaction rate constants. These comparisons reveal that the effect of diffusion on the effective reaction rate constant becomes more profound with time. The time dependent variations in effective reaction rate constant are due to the changes in receptor distribution towards a non-random distribution for high Da numbers ($Da > \sim 0.1$). These comparisons also suggest that well-mixed models are a suitable approach to capture the transients of bimolecular reaction in the plasma membrane for $Da < \sim 0.1$, whereas spatial MC simulation is an appropriate choice, otherwise. Simple PDE models, discussed in this work, cannot accurately capture the transient, effective reaction rate constant of dimerization reaction under all conditions studied. However, the results from such simple PDE models can be used as a quick approximation of the dynamics. The dependence of effective reaction rate constant on instantaneous receptor distribution also has important implications for interpreting experimental data, as discussed in Section 4.1 of Results and discussion.

The Da number criterion, assessed in this work, can provide a simple means for deciding the modeling framework needed for 2D biological systems, such as the plasma membrane. For multi-component, multi-reaction signaling events in the plasma

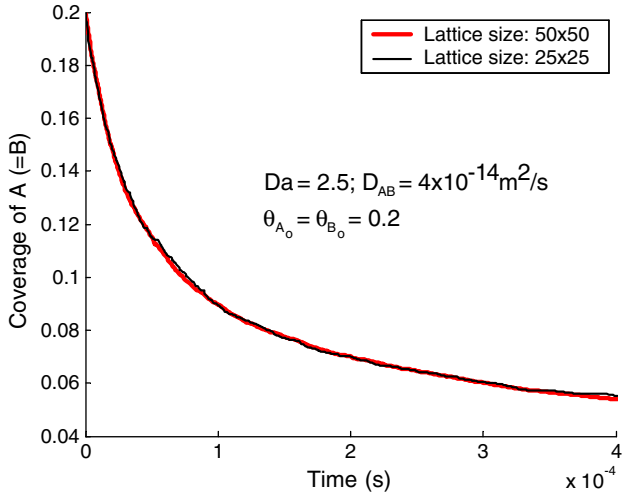

Fig. A1. Comparison of transient coverage profiles of A (=B) for Da=2.5 obtained using two different lattice sizes: 50×50 and 25×25. Curves represent the mean of 10 concentration profiles obtained using different random number seeds.

membrane, estimating the effect of diffusion without detailed spatial modeling can be beneficial. Testing each bimolecular reaction in the plasma membrane using this criterion could be an efficient approach but further work is needed to fully understand complex systems.

In the second part of this work, we used the spatial MC model to explore the effect of spatial heterogeneities, such as localization of receptors in certain regions of the plasma membrane, e.g., lipid rafts, and reduced diffusivities in some regions. Interestingly, our simulations show that localization can dramatically enhance (up to two orders of magnitude) the receptor dimerization rate in cancer cells in comparison to normal cells. This can potentially lead to faster downstream signaling. These results suggest that the spatial features of the plasma membrane should be considered for a realistic realization of the dynamics of intracellular signaling.

In the last part, we have shown that diffusion can influence the noise characteristics of biological networks with redundancy by changing the relative information/mass flow. Overall, this study underscores the importance of stochastic spatial simulations to model stochasticity and spatial heterogeneities of the signaling processes when $Da \sim > 0.1$. This need may be motivated by either the underlying biophysical (such as various membrane heterogeneities) or biochemical (fast reaction kinetics as compared to diffusion) characteristics of the biological events. Furthermore, diffusion, by influencing the relative information flow through various redundant pathways in biological signaling networks, also affects the noise in the number of copies of the signaling proteins.

Finally, MC spatial modeling can generate simulation data which can be compared with data from imaging experiments, such as single particle tracking [99], electron microscopy, FRET and FRAP [67]. A synergistic integration of biophysical, biochemical and imaging data in a computational framework will require MC stochastic spatial modeling for understanding signaling mechanisms.

Acknowledgments

This work was supported by grants from the US Department of Energy (DE-FG02-05ER25702) and the National Science Foundation (CTS-0312117). KM thanks Abhijit Chatterjee, Soumitra Deshmukh and Mark Snyder for useful discussions.

Appendix A

In order to assess that the results of spatial MC simulations are independent of the lattice size, we considered the irreversible dimerization reaction (reaction network 1) at the highest receptor density employed in this study. Simulations at two different lattice sizes, shown in Fig. A1, indicate that indeed our results are statistically independent of the lattice size.

References

[1] U.S. Bhalla, Models of cell signaling pathways, Current Opinion in Genetics and Development 14 (2004) 375–381.
[2] A.R. Asthagiri, D.A. Lauffenburger, Bioengineering models of cell signaling, Annual Review of Biomedical Engineering 2 (2000) 31–53.
[3] B.M. Rao, D.A. Lauffenburger, K.D. Wittrup, Integrating Cell-level Kinetic Modeling Into the Design of Engineered Protein Therapeutics, vol. 23, 2005, pp. 191–194.
[4] M.E. Csete, J.C. Doyle, Reverse engineering of biological complexity, Science 295 (2002) 1664–1669.
[5] H. Kitano, Systems biology: a brief overview, Science 295 (2002) 1662–1664.
[6] A. Ma'ayan, R.D. Blitzer, R. Iyengar, Toward predictive models of mammalian cells, Annual Review of Biophysics and Biomolecular Structure 34 (2005) 319–349.
[7] R. Breitling, D. Hoeller, Current challenges in quantitative modeling of epidermal growth factor signaling, FEBS Letters 579 (2005) 6289–6294.
[8] R.J. Orton, O.E. Sturm, V. Vyshemirsky, M. Calder, D.R. Gilbert, W. Kolch, Computational modelling of the receptor-tyrosine-kinase-activated MAR pathway, Biochemical Journal 392 (2005) 249–261.
[9] H.S. Wiley, S.Y. Shvartsman, D.A. Lauffenburger, Computational modeling of the EGF-receptor system: a paradigm for systems biology, Trends in Cell Biology 13 (2003) 43–50.
[10] C.V. Rao, D.M. Wolf, A.P. Arkin, Control, exploitation and tolerance of intracellular noise, Nature 420 (2002) 231–237.
[11] D. Bray, Signaling complexes: biophysical constraints on intracellular communication, Annual Review of Biophysics and Biomolecular Structure 27 (1998) 59–75.
[12] M. Ehrenberg, J. Elf, E. Aurell, R. Sandberg, J. Tegner, Systems biology is taking off, Genome Research 13 (2003) 2377–2380.
[13] K. Takahashi, S.N.V. Arjunan, M. Tomita, Space in systems biology of signaling pathways — towards intracellular molecular crowding in silico, FEBS Letters 579 (2005) 1783–1788.
[14] D.A. Lauffenburger, J.J. Linderman, Receptors Models for Binding, Trafficking, and Signaling, Oxford University Press, New York, 1993.
[15] S.Y. Shvartsman, H.S. Wiley, W.M. Deen, D.A. Lauffenburger, Spatial range of autocrine signaling: modeling and computational analysis, Biophysical Journal 81 (2001) 1854–1867.
[16] G.C. Brown, B.N. Kholodenko, Spatial gradients of cellular phosphoproteins, FEBS Letters 457 (1999) 452–454.
[17] J. Schaff, C. Fink, B. Slepchenko, J. Carson, L. Loew, A general computational framework for modeling cellular structure and function, Biophysical Journal 73 (1997) 1135–1146.
[18] J. Haugh, D. Lauffenburger, Physical modulation of intracellular signaling processes by locational regulation, Biophysical Journal 72 (1997) 2014–2031.

[19] J.L. Smart, J.A. McCammon, Analysis of synaptic transmission in the neuromuscular junction using a continuum finite element model, Biophysical Journal 75 (1998) 1679–1688.
[20] Y. Song, Y. Zhang, C.L. Bajaj, N.A. Baker, Continuum diffusion reaction rate calculations of wild-type and mutant mouse acetylcholinesterase: adaptive finite element analysis, Biophysical Journal 87 (2004) 1558–1566.
[21] Y. Song, Y. Zhang, T. Shen, C.L. Bajaj, J.A. McCammon, N.A. Baker, Finite element solution of the steady-state Smoluchowski equation for rate constant calculations, Biophysical Journal 86 (2004) 2017–2029.
[22] A. Friboulet, D. Thomas, Reaction diffusion coupling in a structured system — application to the quantitative simulation of end-plate currents, Journal of Theoretical Biology 160 (1993) 441–455.
[23] K. Tai, S.D. Bond, H.R. MacMillan, N.A. Baker, M.J. Holst, J.A. McCammon, Finite element simulations of acetylcholine diffusion in neuromuscular junctions, Biophysical Journal 84 (2003) 2234–2241.
[24] D. Zhang, et al., Tetrameric mouse acetylcholinesterase: continuum diffusion rate calculations by solving the steady-state Smoluchowski equation using finite element methods, Biophysical Journal 88 (2005) 1659–1665.
[25] J.M. Haugh, A unified model for signal transduction reactions in cellular membranes, Biophysical Journal 82 (2002) 591–604.
[26] J. Keizer, J. Ramirez, E. Peacocklopez, The effect of diffusion on the binding of membrane-bound receptors to coated pits, Biophysical Journal 47 (1985) 79–87.
[27] B. Goldstein, C. Wofsy, H. Echavarriaheras, Effect of membrane flow on the capture of receptors by coated pits — theoretical results, Biophysical Journal 53 (1988) 405–414.
[28] B.C. Lagerholm, N.L. Thompson, Theory for ligand rebinding at cell membrane surfaces, Biophysical Journal 74 (1998) 1215–1228.
[29] L. Batsilas, A.M. Berezhkovskii, S.Y. Shvartsman, Stochastic model of autocrine and paracrine signals in cell culture assays, Biophysical Journal 85 (2003) 3659–3665.
[30] M.I. Monine, A.M. Berezhkovskii, E.J. Joslin, H.S. Wiley, D.A. Lauffenburger, S.Y. Shvartsman, Ligand accumulation in autocrine cell cultures, Biophysical Journal 88 (2005) 2384–2390.
[31] M. Pribyl, C.B. Muratov, S.Y. Shvartsman, Discrete models of autocrine cell communication in epithelial layers, Biophysical Journal 84 (2003) 3624–3635.
[32] M. Pribyl, C.B. Muratov, S.Y. Shvartsman, Long-range signal transmission in autocrine relays, Biophysical Journal 84 (2003) 883–896.
[33] D. Shoup, A. Szabo, Role of diffusion in ligand binding to macromolecules and cell-bound receptors, Biophysical Journal 40 (1982) 33–39.
[34] B. Goldstein, M. Dembo, Approximating the effects of diffusion on reversible reactions at the cell surface: ligand–receptor kinetics, Biophysical Journal 68 (1995) 1222–1230.
[35] R. Zwanzig, Diffusion-controlled ligand binding to spheres partially covered by receptors: an effective medium treatment, PNAS 87 (1990) 5856–5857.
[36] H. Berg, E. Purcell, Physics of chemoreception, Biophysical Journal 20 (1977) 193–219.
[37] B. Goldstein, R. Posner, D. Torney, J. Erickson, D. Holowka, B. Baird, Competition between solution and cell surface receptors for ligand. Dissociation of hapten bound to surface antibody in the presence of solution antibody, Biophysical Journal 56 (1989) 955–966.
[38] A.A. Potanin, V. Vladyslav, O.S. Belokoneva, F.W. Wiegel, Kinetics of ligand binding to a cluster of membrane-associated receptors, European Biophysics Journal (Historical Archive) 23 (1994) 197–205.
[39] J. Erickson, B. Goldstein, D. Holowka, B. Baird, The effect of receptor density on the forward rate constant for binding of ligands to cell surface receptors, Biophysical Journal 52 (1987) 657–662.
[40] D. Wang, S.-Y. Gou, D. Axelrod, Reaction rate enhancement by surface diffusion of adsorbates, Biophysical Chemistry 43 (1992) 117–137.
[41] R. Zwanzig, A. Szabo, Time dependent rate of diffusion-influenced ligand binding to receptors on cell surfaces, Biophysical Journal 60 (1991) 671–678.
[42] I.M. Sokolov, H. Schnorer, A. Blumen, Diffusion-controlled reaction A $+B \rightarrow 0$ in one dimension — the role of particle mobilities and the diffusion-equation approach, Physical Review A 44 (1991) 2388–2393.
[43] D.C. Torney, H.M. McConnell, Diffusion-limited reactions in one dimension, Journal of Physical Chemistry 87 (1983) 1941–1951.
[44] K. Lindenberg, P. Argyrakis, R. Kopelman, Reaction–diffusion model for A+A reaction, Journal of Physical Chemistry 99 (1995) 7542–7556.
[45] A.V. Barzykin, K. Seki, M. Tachiya, Kinetics of diffusion-assisted reactions in microheterogeneous systems, Advances in Colloid and Interface Science 89 (2001) 47–140.
[46] J. Keizer, Diffusion effects on rapid bimolecular chemical-reactions, Chemical Reviews 87 (1987) 167–180.
[47] M.V. Smoluchowski, Versuch einer mathematischen Theorie der Koagulationskinetik kolloider Lösungen, Zeitschrift für Physikalische Chemie 92 (1917) 129–168.
[48] A. Szabo, R. Zwanzig, N. Agmon, Diffusion-controlled reactions with mobile traps, Physical Review Letters 61 (1988) 2496–2499.
[49] F.C. Collins, G.E. Kimball, Diffusion-controlled reaction rates, Journal of Colloid Science 4 (1949) 425–437.
[50] J.W. Cahn, J.E. Hilliard, Free energy of a nonuniform system: I. Interfacial free energy, Journal of Chemical Physics 28 (1958) 258–267.
[51] A. Chatterjee, M.A. Snyder, D.G. Vlachos, Mesoscopic modeling of chemical reactivity, Chemical Engineering Science 59 (2004) 5559–5567.
[52] D.C. Torney, H.M. McConnell, Diffusion-limited reaction theory for two-dimensional systems, Proceedings of the Royal Society of London. A 387 (1983) 147–170.
[53] G. Lamm, K. Schulten, Extended Brownian dynamics approach to diffusion-controlled processes, Journal of Chemical Physics 75 (1981) 365–371.
[54] G. Lamm, K. Schulten, Extended Brownian dynamics: 2. Reactive, non-linear diffusion, Journal of Chemical Physics 78 (1983) 2713–2734.
[55] S.H. Northrup, S.A. Allison, J.A. McCammon, Brownian dynamics simulation of diffusion-influenced bimolecular reactions, Journal of Chemical Physics 80 (1984) 1517–1526.
[56] S.H. Northrup, M.S. Curvin, S.A. Allison, J.A. McCammon, Optimization of Brownian dynamics methods for diffusion-influenced rate-constant calculations, Journal of Chemical Physics 84 (1986) 2196–2203.
[57] N. Agmon, A. Edelstein, Collective binding properties of receptor arrays, Biophysical Journal 72 (1997) 1582–1594.
[58] R.C. Wade, Brownian dynamics simulations of enzyme–substrate encounter, Biochemical Society Transactions 24 (1996) 254–259.
[59] J.A. McCammon, S.H. Northrup, S.A. Allison, Diffusional dynamics of ligand receptor association, Journal of Physical Chemistry 90 (1986) 3901–3905.
[60] H.X. Zhou, Kinetics of diffusion-influenced reactions studied by Brownian dynamics, Journal of Physical Chemistry 94 (1990) 8794–8800.
[61] N. Agmon, A.L. Edelstein, The long-time behavior of reversible binary reactions — theory, Brownian simulations and experiment, Journal of Chemical Physics 100 (1994) 4181–4187.
[62] N. Agmon, A. Szabo, Theory of reversible diffusion-influenced reactions, Journal of Chemical Physics 92 (1990) 5270–5284.
[63] R.R. Gabdoulline, R.C. Wade, Brownian dynamics simulation of protein–protein diffusional encounter, Methods 14 (1998) 329–341.
[64] G. Zou, R.D. Skeel, Robust biased Brownian dynamics for rate constant calculation, Biophysical Journal 85 (2003) 2147–2157.
[65] M.I. Monine, J.M. Haugh, Reactions on cell membranes: comparison of continuum theory and Brownian dynamics simulations, The Journal of Chemical Physics 123 (2005) 074908.
[66] B.M. Slepchenko, J.C. Schaff, J.H. Carson, L.M. Loew, Computational cell biology: spatiotemporal simulation of cellular events, Annual Review of Biophysics and Biomolecular Structure 31 (2002) 423–441.
[67] C. Lemerle, B.D. Ventura, L. Serrano, Space as the final frontier in stochastic simulations of biological systems, FEBS Letters 579 (2005) 1789–1794.

[68] S.S. Andrews, D. Bray, Stochastic simulation of chemical reactions with spatial resolution and single molecule detail, Physical Biology 1 (2004) 137–151.
[69] L. Shea, G. Omann, J. Linderman, Calculation of diffusion-limited kinetics for the reactions in collision coupling and receptor cross-linking, Biophysical Journal 73 (1997) 2949–2959.
[70] J.R. Stiles Jr., T.M.B., E.E. Salpeter, M.M. Salpeter, in: J.M. Bower (Ed.), Computational Neuroscience, Plenum, New York, 1998, pp. 279–284.
[71] J.S. Reese, S. Raimondeau, D.G. Vlachos, Monte Carlo algorithms for complex surface reaction mechanisms: efficiency and accuracy, Journal of Computational Physics 173 (2001) 302–321.
[72] T.S. Shimizu, S.V. Aksenov, D. Bray, A spatially extended stochastic model of the bacterial chemotaxis signalling pathway, Journal of Molecular Biology 329 (2003) 291–309.
[73] J.R. Stiles, T.M. Bartol, Monte Carlo methods for simulating realistic synaptic micro-physiology using MCell, in: E.D. Schutter (Ed.), Computational Neuroscience: Realistic Modeling for Experimentalists, CRC Press, New York, 2000.
[74] M.R. Bennett, L. Farnell, W.G. Gibson, The probability of quantal secretion near a single calcium channel of an active zone, Biophysical Journal 78 (2000) 2201–2221.
[75] A. Chatterjee, K. Mayawala, J.S. Edwards, D.G. Vlachos, Time accelerated Monte Carlo simulations of biological networks using the binomial {tau}-leap method, Bioinformatics 21 (2005) 2136–2137.
[76] H. Resat, J.A. Ewald, D.A. Dixon, H.S. Wiley, An integrated model of epidermal growth factor receptor trafficking and signal transduction, Biophysical Journal 85 (2003) 730–743.
[77] L. Salwinski, D. Eisenberg, In silico simulation of biological network dynamics, Nature Biotechnology 22 (2004) 1017–1019.
[78] E.M. Ozbudak, M. Thattai, I. Kurtser, A.D. Grossman, A.v. Oudenaarden, Regulation of noise in the expression of a single gene, Nature Genetics 31 (2002) 69–73.
[79] H. Salis, Y. Kaznessis, Accurate hybrid stochastic simulation of a system of coupled chemical or biochemical reactions, Journal of Chemical Physics 122 (2005).
[80] M.B. Elowitz, A.J. Levine, E.D. Siggia, P.S. Swain, Stochastic gene expression in a single cell, Science 297 (2002) 1183–1186.
[81] W.J. Blake, M. Kaern, C.R. Cantor, J.J. Collins, Noise in eukaryotic gene expression, Nature 422 (2003) 633–637.
[82] G. Vereb, et al., Dynamic, yet structured: the cell membrane three decades after the Singer–Nicolson model, PNAS 100 (2003) 8053–8058.
[83] K. Murase, et al., Ultrafine membrane compartments for molecular diffusion as revealed by single molecule techniques, Biophysical Journal 86 (2004) 4075–4093.
[84] H. Murakoshi, R. Iino, T. Kobayashi, T. Fujiwara, C. Ohshima, A. Yoshimura, A. Kusumi, Single-molecule imaging analysis of Ras activation in living cells, PNAS 101 (2004) 7317–7322.
[85] B.S. Wilson, et al., Markers for detergent-resistant lipid rafts occupy distinct and dynamic domains in native membranes, Molecular Biology of the Cell 15 (2004) 2580–2592.
[86] F.R. Maxfield, Plasma membrane microdomains, Current Opinion in Cell Biology 14 (2002) 483–487.
[87] P.H.M. Lommerse, H.P. Spaink, T. Schmidt, In vivo plasma membrane organization: results of biophysical approaches, Biochimica et Biophysica Acta (BBA) — Biomembranes 1664 (2004) 119–131.
[88] A.J. Laude, I.A. Prior, Plasma membrane microdomains: organization, function and trafficking (Review), Molecular Membrane Biology 21 (2004) 193–205.
[89] A. Kusumi, et al., Paradigm shift of the plasma membrane concept from the two-dimensional continuum fluid to the partitioned fluid: high-speed single-molecule tracking of membrane molecules, Annual Review of Biophysics and Biomolecular Structure 34 (2005) 351–378.
[90] K. Simons, D. Toomre, Lipid rafts and signal transduction, Nature Reviews Molecular Cell Biology 1 (2000) 31–39.
[91] L.J. Pike, Lipid rafts: bringing order to chaos, Journal of Lipid Research 44 (2003) 655–667.
[92] D.S. Lidke, P. Nagy, R. Heintzmann, D.J. Arndt-Jovin, J.N. Post, H.E. Grecco, E.A. Jares-Erijman, T.M. Jovin, Quantum dot ligands provide new insights into erbB/HER receptor-mediated signal transduction, Nature Biotechnology 22 (2004) 198–203.
[93] M. Thattai, A. van Oudenaarden, Intrinsic noise in gene regulatory networks, PNAS 98 (2001) 8614–8619.
[94] M. Kærn, W.J. Blake, J.J. Collins, The engineering of gene regulatory networks, Annual Review of Biomedical Engineering 5 (2003) 179–206.
[95] W. Bialek, S. Setayeshgar, Physical limits to biochemical signaling, PNAS 102 (2005) 10040–10045.
[96] U.S. Bhalla, Signaling in small subcellular volumes: I. Stochastic and diffusion effects on individual pathways, Biophysical Journal 87 (2004) 733–744.
[97] U.S. Bhalla, Signaling in small subcellular volumes: II. Stochastic and diffusion effects on synaptic network properties, Biophysical Journal 87 (2004) 745–753.
[98] R. Metzler, The future is noisy: the role of spatial fluctuations in genetic switching, Physical Review Letters 87 (2001) 068103.
[99] K. Mayawala, D.G. Vlachos, J.S. Edwards, Computational modeling reveals molecular details of epidermal growth factor binding, BMC Cell Biology 6 (2005) 41.
[100] B. Schoeberl, C. Eichler-Jonsson, E.D. Gilles, G. Müller, Computational modeling of the dynamics of the MAP kinase cascade activated by surface and internalized EGF receptors, Nature Biotechnology 20 (2002) 370–375.
[101] E. Jakobsson, Computer simulation studies of biological membranes: progress, promise and pitfalls, Trends in Biochemical Sciences 22 (1997) 339–344.
[102] Kirk-Othmer, Kirk-Othmer Encyclopedia of Chemical Technology, Wiley, 1999.
[103] C.L. Roy, J.L. Wrana, Clathrin- and non-clathrin-mediated endocytic regulation of cell signalling, Nature Reviews Molecular Cell Biology 6 (2005) 112–126.
[104] D.G. Vlachos, A review of multiscale analysis: examples from systems biology, materials engineering, and other fluid–surface interacting systems, Advances in Chemical Engineering 30 (2005) 1–61.
[105] P. Mahama, J. Linderman, A Monte Carlo study of the dynamics of G-protein activation, Biophysical Journal 67 (1994) 1345–1357.
[106] H. Wiley, Anomalous binding of epidermal growth factor to A431 cells is due to the effect of high receptor densities and a saturable endocytic system, Journal of Cell Biology 107 (1988) 801–810.
[107] M. Benveniste, E. Livneh, J. Schlessinger, Z. Kam, Overexpression of epidermal growth factor receptor in NIH-3T3-transfected cells slows its lateral diffusion and rate of endocytosis, Journal of Cell Biology 106 (1988) 1903–1909.
[108] K. Jacobson, E.D. Sheets, R. Simson, Revisiting the fluid mosaic model of membranes, Science 268 (1995) 1441–1442.
[109] A. Kusumi, Y. Sako, Cell surface organization by the membrane skeleton, Current Opinion in Cell Biology 8 (1996) 566–574.
[110] L.D. Zajchowski, S.M. Robbins, Lipid rafts and little caves. Compartmentalized signalling in membrane microdomains, European Journal of Biochemistry 269 (2002) 737–752.
[111] R.G. Parton, J.F. Hancock, Lipid rafts and plasma membrane microorganization: insights from Ras, Trends in Cell Biology 14 (2004) 141–147.
[112] K. Mayawala, D.G. Vlachos, J.S. Edwards, Heterogeneities in EGF receptor density at the cell surface can lead to concave up Scatchard plot of EGF binding, FEBS Letters 579 (2005) 3043–3047.
[113] A. Kusumi, Y. Sako, M. Yamamoto, Confined lateral diffusion of membrane receptors as studied by single particle tracking (nanovid microscopy). Effects of calcium-induced differentiation in cultured epithelial cells, Biophysical Journal 65 (1993) 2021–2040.
[114] F. Wiegant, F. Blok, L. Defize, W. Linnemans, A. Verkley, J. Boonstra, Epidermal growth factor receptors associated to cytoskeletal elements of epidermoid carcinoma (A431) cells, Journal of Cell Biology 103 (1986) 87–94.
[115] A. Pralle, P. Keller, E.-L. Florin, K. Simons, J.K.H. Horber, Sphingolipid-cholesterol rafts diffuse as small entities in the plasma membrane of mammalian cells, Journal of Cell Biology 148 (2000) 997–1008.

[116] B.N. Kholodenko, Four-dimensional organization of protein kinase signaling cascades: the role of diffusion, endocytosis, molecular motors, The Journal of Experimental Biology 206 (2003) 2073–2082.
[117] J. Elf, M. Ehrenberg, Fast evaluation of fluctuations in biochemical networks with the linear noise approximation, Genome Research 13 (2003) 2475–2484.
[118] D. Orrell, S. Ramsey, P. de Atauri, H. Bolouri, A method for estimating stochastic noise in large genetic regulatory networks, Bioinformatics 21 (2005) 208–217.
[119] G.M. Edelman, J.A. Gally, Degeneracy and complexity in biological systems, PNAS 98 (2001) 13763–13768.
[120] H.H. McAdams, A. Arkin, It's a noisy business! Genetic regulation at the nanomolar scale, Trends in Genetics 15 (1999) 65–69.
[121] D.L. Cook, A.N. Gerber, S.J. Tapscott, Modeling stochastic gene expression: implications for haploinsufficiency, PNAS 95 (1998) 15641–15646.